

Sensored (Hall Effect Sensor-Based) Field Oriented Control of Three-Phase BLDC Motor Using dsPIC33CK

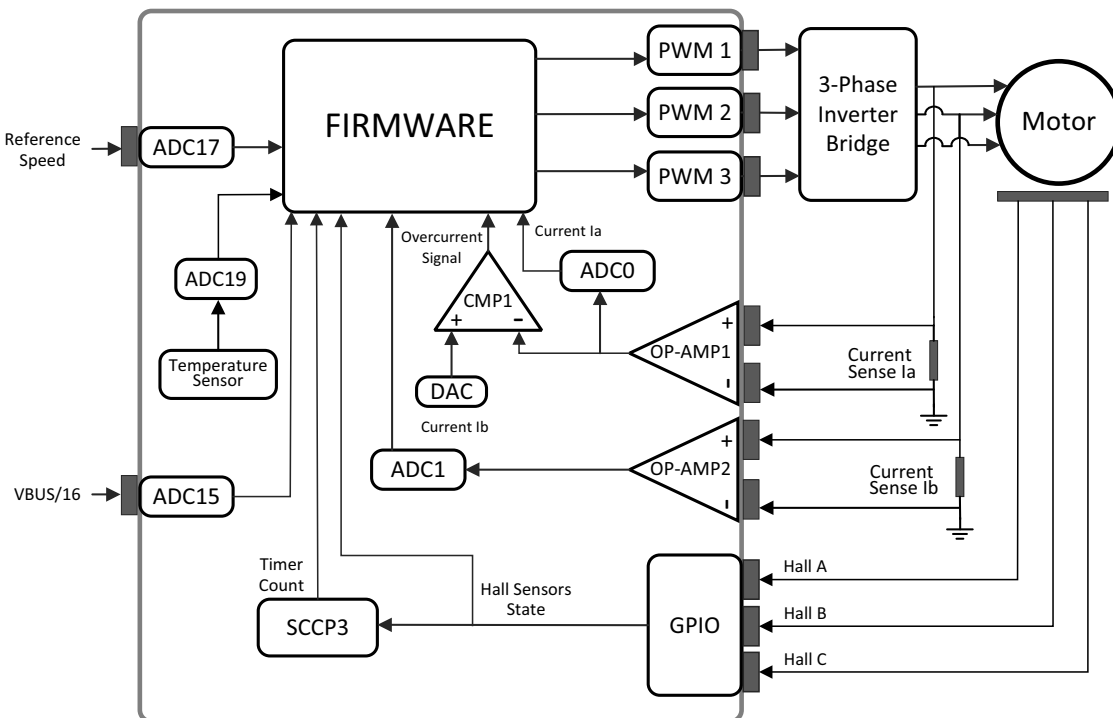
Author: Maria Loida Canada

Introduction

The construction of modern BLDC motors allows them to be controlled like permanent magnet synchronous motors. This means that a sophisticated technique called Field Oriented Control (FOC) is also applicable to BLDC motors. The FOC algorithm is useful in the applications that require fast dynamic response with independent control of torque and flux. Sensor-based FOC is advantageous for providing rotor position at slower speeds.

This application note describes the implementation of a Hall effect sensor-based FOC algorithm for three-phase BLDC motors using Microchip Technology's 16-bit dsPIC33CK DSC's. The mathematical computations and transformations are performed by the DSP engine, while the on-chip peripherals, such as PWM, SCCP, op amps, Comparator with DAC, simplify the implementation and reduce the overall system components. The following figure shows the block diagram of the solution.

FIGURE 1: SYSTEM BLOCK DIAGRAM

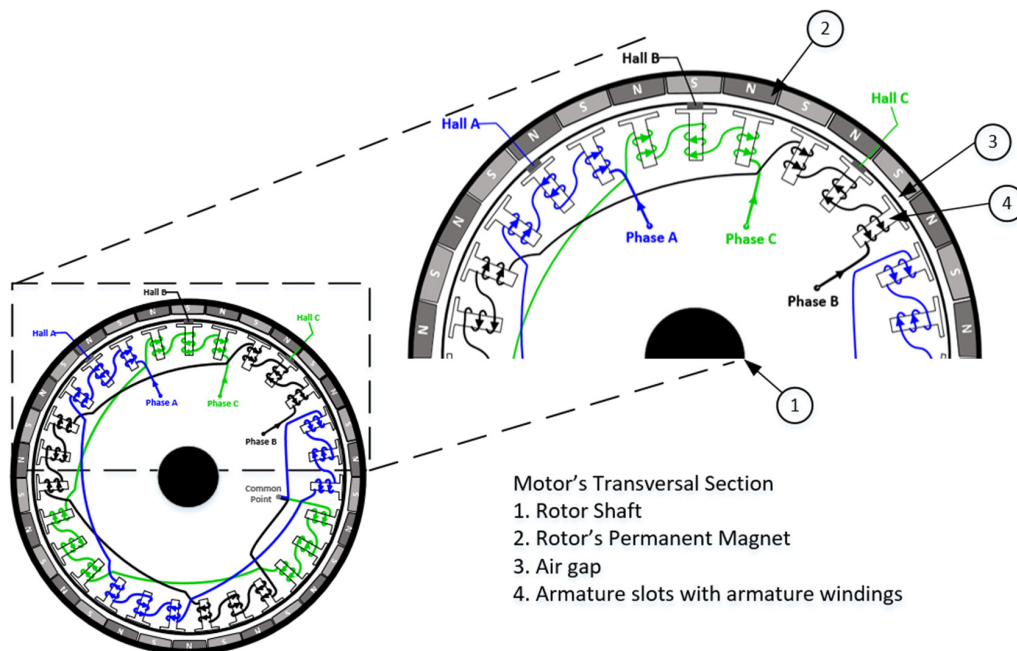


1.0 FIELD ORIENTED CONTROL IN SENSORED BLDC

Field Oriented Control is a commutation method that keeps the rotor and stator magnetic fields at 90 degrees under all conditions, enabling maximum torque generation from the motor and regulation of speed/torque under changing load conditions. It deals with the fluxes (stator, rotor or air-gap). One of those is used as a reference frame for all other quantities with the purpose of decoupling the torque- and flux- producing components of current. The decoupling ensures the ease of control of the three-phase motor, similar to the DC motor with separate excitation. This means that the armature current is responsible for the torque generation, and the excitation current is responsible for the flux generation. In this application, the rotor flux is used as a reference frame.

The air-gap flux is equal to the sum of the rotor's flux linkage, which is generated by the permanent magnets plus the armature reaction flux linkage generated by the stator current. The air-gap flux for this motor is smooth, and the Back Electromagnetic Force (BEMF) is sinusoidal. This control scheme is created for the sensored BLDC motor that is used as a hub motor in electric scooters. The motor's transversal section is shown in the following figure.

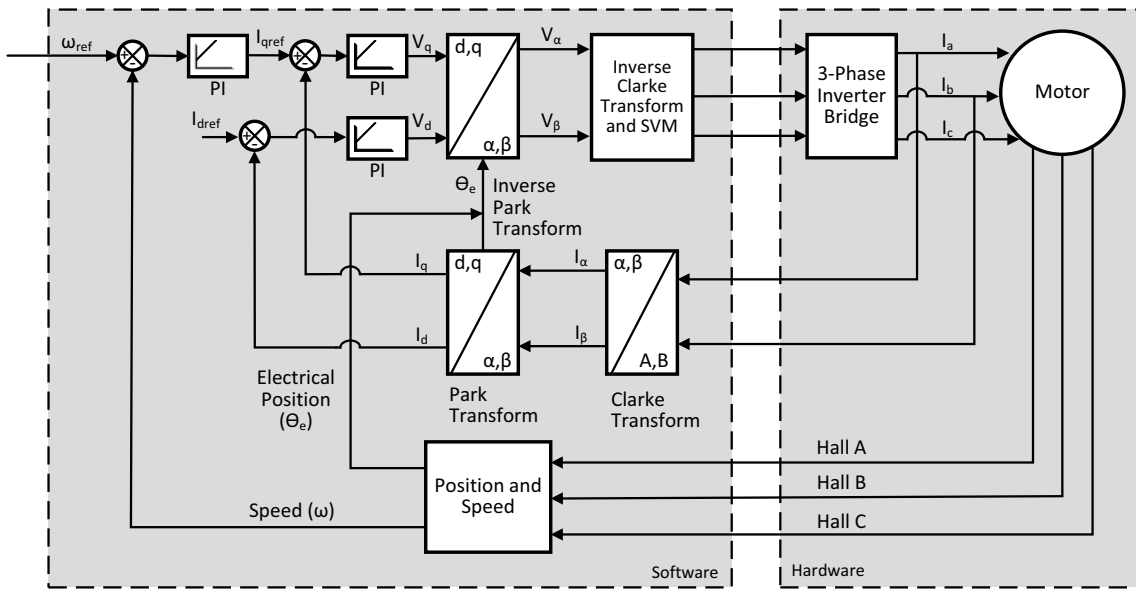
FIGURE 2: MOTOR'S TRANSVERSAL SECTION



For applications requiring precise control or high torque generation at low motor speeds, sensored control is preferred. In the sensored FOC implementation, rotor position and speed are determined using an encoder, resolver or Hall effect sensors. This application note describes the Hall sensor-based implementation with the target application in driving electric scooter hub motors.

2.0 BLOCK DIAGRAM OF SENSORED FOC

FIGURE 3: FOC BLOCK DIAGRAM



The control process in the previous figure can be summarized as follows:

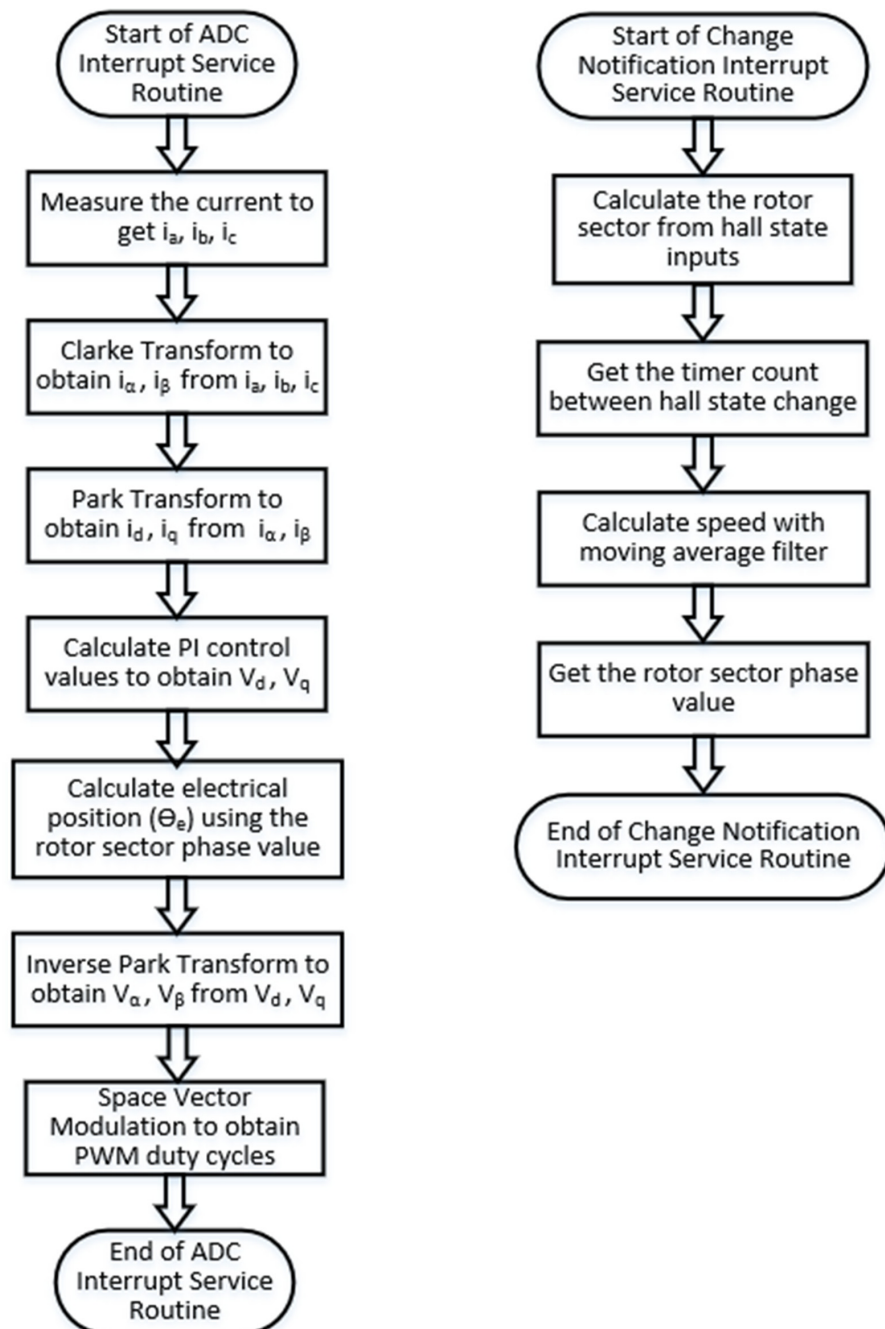
- The three-phase stator currents are measured. For a motor with balanced three-phase windings, only two phase currents are sufficient to be measured. The third current is calculated using the following equation: $i_a + i_b + i_c = 0$.
- Clarke Transform: The three-phase currents are converted to a stationary two-axis system. The conversion provides the variables i_α and i_β from the measured i_a and i_b values. The values i_α and i_β are time varying quadrature current values as viewed from the perspective of the stator.
- Park Transform: The stationary two-axis coordinate system is rotated to align with the rotor flux using a transformation based on the angle measured at the last iteration of the control loop. This conversion provides the i_d and i_q variables from i_α and i_β . The variables i_d and i_q are the quadrature currents transformed to the rotating coordinate system. For steady state conditions, i_d and i_q are constant.
- Reference values of currents are defined as follows;
 - i_d reference: controls rotor magnetizing flux
 - i_q reference: controls the torque output of the motor
- The error signals are fed to PI controllers. The output of the controllers provide v_d and v_q , which are the voltage vectors that will be applied to the motor.
- A new transformation angle is measured and calculated based on the Hall sensor's state. The new angle guides the FOC algorithm as to where to place the next voltage vector.
- Inverse Park Transform: The v_d and v_q output values from the PI controllers are rotated back to the stationary reference frame using the new angle. This calculation provides the succeeding quadrature voltage values v_α and v_β .
- Inverse Clarke Transform and SVM: The v_α and v_β values are used to calculate the new PWM duty cycle values, which will generate the desired voltage vector.
- The speed (ω) is calculated with every Hall state change, which happens after every discrete PWM cycle.

The FOC firmware is implemented in the ADC Interrupt Service Routine (ISR), which runs at the same rate as the PWM switching frequency.

3.0 FLOWCHART OF SENSORED FOC

The flowchart in the following figure shows the equivalent sequential routine of the FOC in software, and the change notification routine used for measuring the speed and rotor position. The complete source code of the solution can be found in [Appendix A: “Source Code Listing”](#).

FIGURE 4: FLOWCHART



4.0 PI CONTROLLER

4.1 PI Controller Background

A complete discussion about the Proportional Integral (PI) controllers is beyond the scope of this document. However, this section provides some basics of PI operation.

A PI controller responds to an error signal in a closed control loop, and attempts to adjust the controlled quantity to achieve the desired system response. The controlled parameter can be any measurable system quantity, such as speed or flux. The benefit of the PI controller is that it can be adjusted empirically by varying one or more gain values and observing the change in the system response.

A digital PI controller is executed at a periodic sampling interval. It is assumed that the controller is executed frequently, hence the system can be controlled. The error signal is formed by subtracting the desired setting of the parameter to be controlled from the actual measured value of that parameter. The sign of the error indicates the direction of change required by the control input.

The Proportional (P) term of the controller is formed by multiplying the error signal by a 'P' gain, causing the PI controller to produce a control response, which is a function of the error magnitude. As the error signal becomes larger, the 'P' term of the controller becomes larger to provide more correction.

The effect of the 'P' term tends to reduce the overall error as time elapses. However, the effect of the 'P' term diminishes as the error approaches zero. With proportional control, in most systems, the error of the controlled parameter gets very close to zero but does not converge. The result is a small remaining steady state error.

The Integral 'I' term of the controller is used to eliminate small steady state errors. The 'I' term calculates a continuous running total of the error signal. Therefore, a small steady state error accumulates into a large error value over time. This accumulated error signal is multiplied by an 'I' gain factor and becomes the 'I' output term of the PI controller.

4.2 Adjusting PI Gains

The 'P' gain of a PI controller sets the overall system response. To tune the controller, set the 'I' gain to zero. Then, increase the 'P' gain until the system responds to set point changes without excessive overshoot or oscillations. Using lower values of 'P' gain will slowly control the system, while higher values will give aggressive control. At this point, the system will probably not converge to the set point.

After a reasonable 'P' gain is selected, slowly increase the 'I' gain to force the system error to zero. Only a small amount of 'I' gain is required in most systems. The effect of the 'I' gain, if large enough, can overcome the action of the 'P' term, slow the overall control response and cause the system to oscillate around the set point. If oscillation occurs, reducing the 'I' gain and increasing the 'P' gain will usually solve the problem.

This application includes a term to limit the integral windup, which occurs if the integrated error saturates the output parameter. Any further increase in the integrated error does not affect the output. The accumulated error, when it does decrease, will have to fall (or unwind) to below the value that caused the output to saturate.

There are three PI control loops used to control the three interactive variables in this application. The outer loop controls the rotor speed; the two inner loops control the rotor flux and the motor torque, respectively.

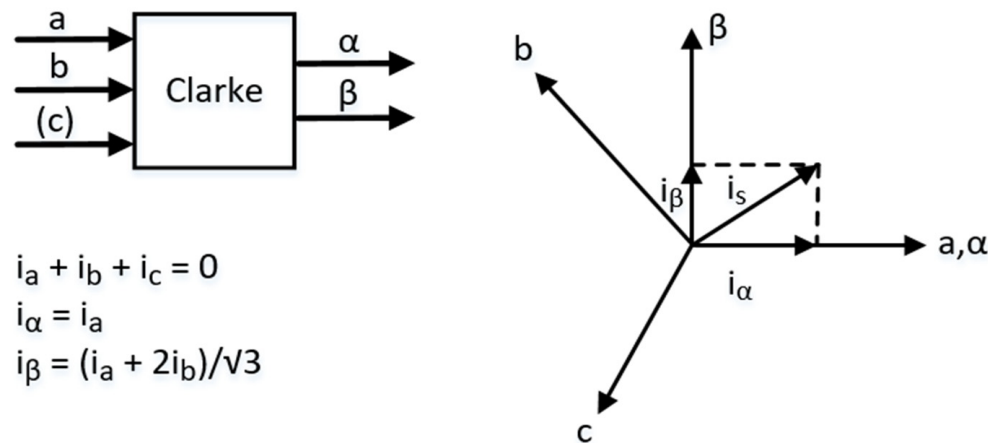
5.0 COORDINATE TRANSFORMS

Through a series of coordinate transforms, users can indirectly determine and control the time invariant values of torque and flux with classic PI control loops. The process begins by measuring the 3-phase motor currents. In practice, the instantaneous sum of the three current values is zero due to the balance phase windings. Therefore, by measuring only two of the three phase currents, the third will be determined, which reduces hardware costs by eliminating the need for the third current sensor.

5.1 Clarke Transform

The Clarke Transform transforms the quantities from the three-axis, two-dimensional coordinate system referenced to the stator, to a two-axis stationary coordinate system.

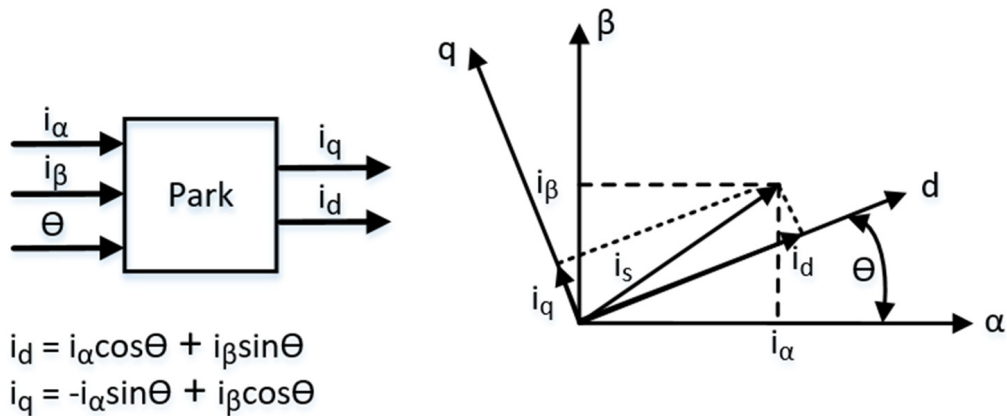
FIGURE 5: CLARKE TRANSFORM



5.2 Park Transform

The Park Transform transforms the quantities from the two-axis stationary coordinate system to a two-axis rotating coordinate system that rotates with the rotor flux. Theta is the angle of the rotor flux from the stationary reference frame.

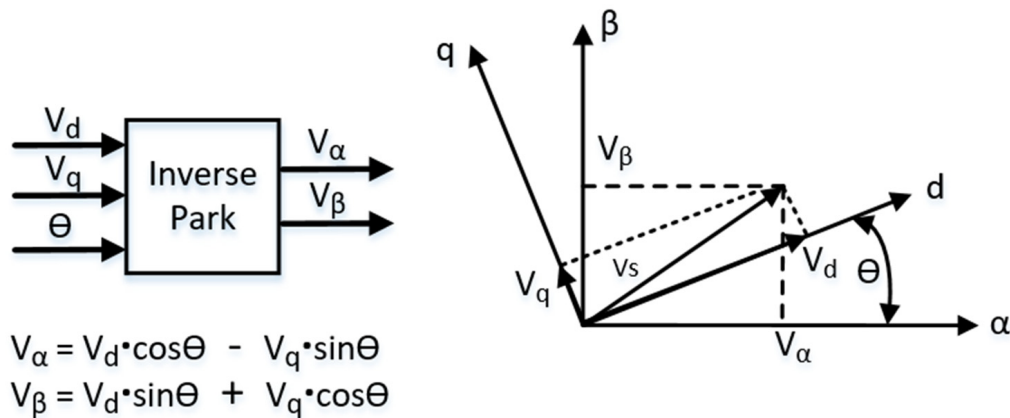
FIGURE 6: PARK TRANSFORM



5.3 Inverse Park Transform

The Inverse Park Transform transforms the quantities from the two-axis rotating coordinate system that rotates with the rotor flux, to a two-axis stationary coordinate system.

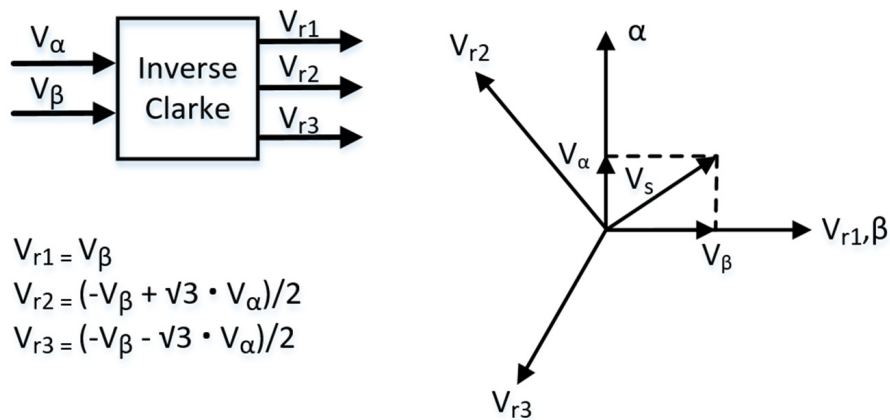
FIGURE 7: INVERSE PARK TRANSFORM



5.4 Inverse Clarke Transform

The Inverse Clarke Transform transforms the quantities from a two-axis stationary coordinate system to a three-axis, two-dimensional coordinate system referenced to the stator. The alpha and beta axes are interchanged from that of a conventional Inverse Clarke transform to simplify the SVPWM implementation, which will be further discussed in the next section.

FIGURE 8: INVERSE CLARKE TRANSFORM



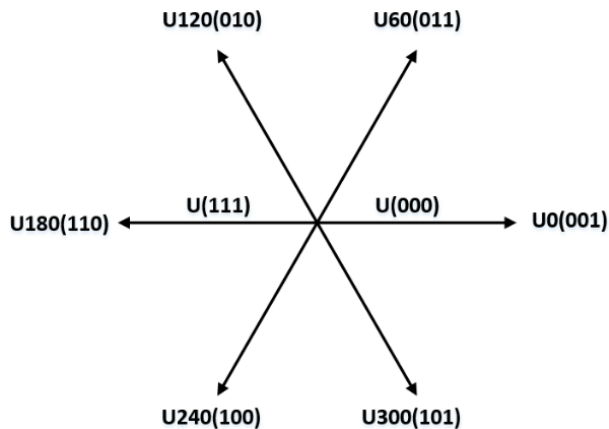
6.0 SPACE VECTOR PULSE WIDTH MODULATION (SVPWM)

The final step in the vector control process is to generate pulse-width modulation signals for the 3-phase motor voltages. If the Space Vector Modulation (SVM) technique is used, the process of generating the pulse width for each of the three phases is reduced to a few simple equations. In this implementation, the Inverse Clarke Transform is folded into the SVM routine, which further simplifies the calculations.

Each of the three inverter outputs can be in one of two states. The inverter output can be connected to either the plus (+) bus rail or the minus (-) bus rail, which allows for $2^3 = 8$ possible states of the output.

The two states in which all three outputs are connected to either the plus (+) bus or the minus (-) bus are considered null states because there is no line-to-line voltage across any of the phases. These are plotted at the origin of the SVM star. The remaining six states are represented as vectors with a 60-degree phase difference between the adjacent states.

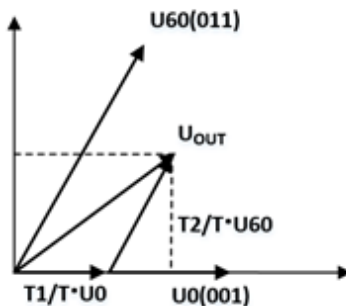
FIGURE 9: SPACE VECTORS OF THREE-PHASE INVERTER



The process of SVM allows the representation of any resultant vector by the sum of the components of the two adjacent vectors. In the figure below, U_{OUT} is the desired resultant. It lies in the sector between U_{60} and U_0 . If during a given PWM period T , U_0 is output for T_1 / T and U_{60} is output for T_2 / T , the resulting voltage for the period T will be U_{OUT} .

FIGURE 10: AVERAGE SVPWM

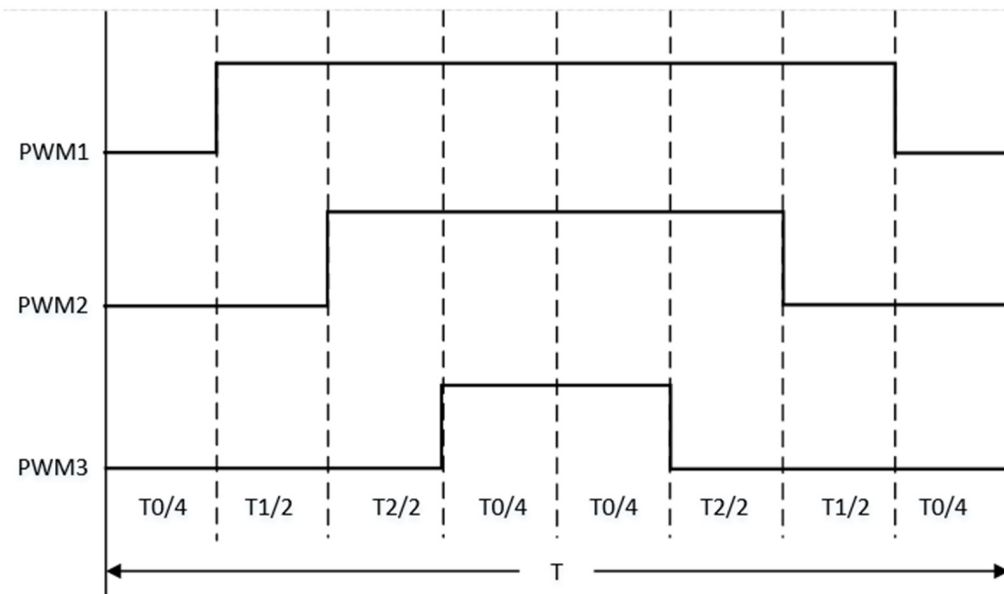
T_0 = Null Vector
 $T = T_1 + T_2 + T_0$ = PWM Period
 $U_{OUT} = (T_1/T \cdot U_0) + (T_2/T \cdot U_{60})$



T_0 represents a time where no effective voltage is applied into the windings; i.e., where a null vector is applied. The values for T_1 and T_2 can be extracted with no extra calculations by using a modified Inverse Clarke transformation. If V_α and V_β are reversed, a reference axis is generated that is shifted by 30 degrees from the SVM star. As a result, for each of the six segments, one axis is exactly opposite that segment and the other two axes symmetrically bound that segment. The timings of the vector components along those two bounding axes are equal to T_1 and T_2 . The null vectors are applied in the remaining time T_0 of the switching period T .

The dsPIC DSC is configured in the center-aligned PWM, which produces the symmetrical pulse pattern as shown in the following figure. This configuration reduces the ripple current while minimizing the switching losses in the power device.

FIGURE 11: PWM SIGNALS FOR PERIOD T

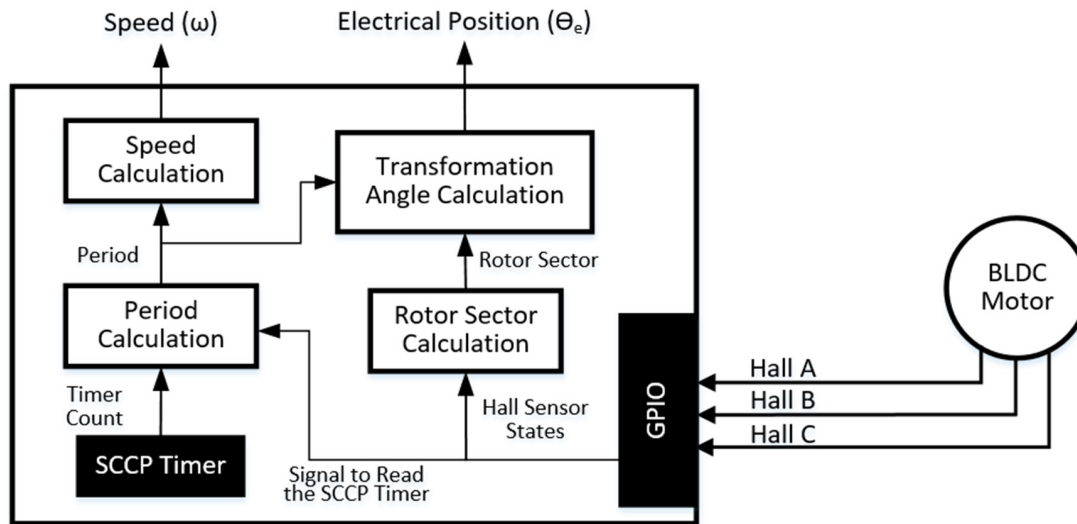


7.0 SENSORED IMPLEMENTATION OF POSITION AND SPEED MEASUREMENT

An important part of the algorithm is how to calculate the rotor angle needed for the FOC. This section of the application note explains the process of estimating the rotor angle (Θ) and motor speed (ω). The sensored control technique estimates those parameters from the information obtained from the discrete states of the Hall sensor inputs.

The block diagram of the position and speed measurement is shown in the following figure. The sensored technique uses the GPIO and SCCP (Capture/Compare/PWM/Timer) peripherals. The GPIO with Change Notification feature is configured with mismatch style, which means that it detects changes from the last port read. The SCCP peripheral is configured into Timer mode, using the FCY Clock of 100 MHz and prescaler of 64. The SCCP Timer period is based on the minimum motor speed to avoid overflow and accommodate the maximum period.

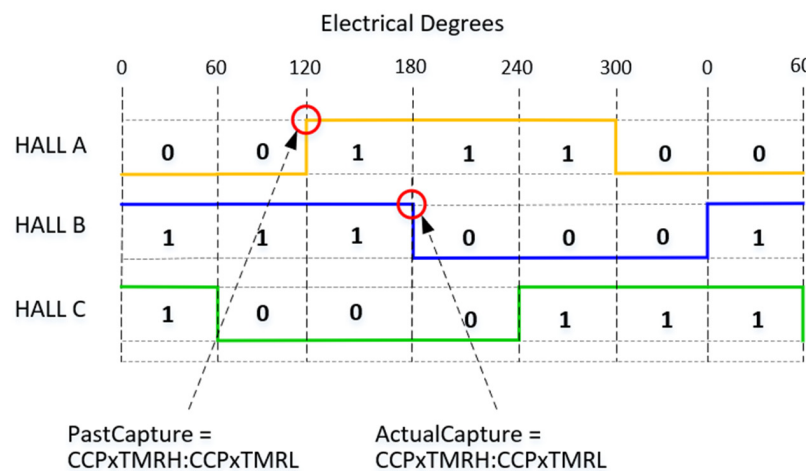
FIGURE 12: POSITION AND SPEED MEASUREMENT DIAGRAM



Whenever the motor rotates, there is a Hall state change, which happens every 60 electrical degrees, the Change Notification ISR (CN_ISR()) is serviced. Within the ISR, the Hall sensor's state is read, and the rotor sector is calculated. The interrupt event also measures the timer count of the SCCP Timer between subsequent interrupts.

The following figure illustrates the Hall states and its changes that trigger the interrupt events. The period calculation is done by measuring the current timer count (ActualCapture) and subtracting it from the previous timer count (PastCapture). The calculated period is filtered using the moving average filtering method. The moving average filtering method is optimal for reducing random noise while maintaining a sharp response. It is done by getting multiple period samples at a time, and taking the average of those to produce a single output point. The average period is used in calculating the rotor position, while the raw calculated period is passed to the speed calculation routine.

FIGURE 13: TIMER COUNT CAPTURE FOR PERIOD CALCULATION



7.1 Position Measurement

It is important to know the accurate rotor position for the FOC to work correctly. The low-resolution discrete inputs from the Hall effect sensor states would not be sufficient for the FOC because it requires a higher angle resolution to properly execute the control.

The rotor sector is needed to properly get the rotor sector phase value. Rotor sector is the absolute position of the rotor, in electrical degrees, in 60-degree steps. That information is obtained by reading the digital value from the three Hall effect sensors. There are six valid sectors that are assigned with corresponding phase values in signed integer format. The values are tabulated in the following table with the corresponding Hall state and sector number.

TABLE 1: RELATIONSHIP OF SECTOR TO ANGULAR POSITION

Hall C	Hall B	Hall A	Sector	Reference Phase Value
0	0	0	Invalid	Invalid
1	1	0	6	32767
0	1	0	2	-21844
0	1	1	3	-10922
0	0	1	1	0
1	0	1	5	10922
1	0	0	4	21844
1	1	1	Invalid	Invalid

The phase values serve as references to calculate the high-resolution transformation angle. The reference phase value based on the sector is acquired with every change notification interrupt event, while the calculation of the transformation angle is done in ADC_ISR(). The reference phase value is initially loaded to the transformation angle within the CN_ISR(), given by the following equation.

EQUATION 1: INITIAL TRANSFORMATION ANGLE

$$\text{thetaElectrical} = \text{Reference Phase Value} + \text{_90_Degrees_Phase_Offset}$$

The `_90_Degrees_Phase_Offset` keeps the stator and rotor flux at 90 degrees from each other. It is equivalent to 16384 and computed from the whole electrical angle rotation of 65536.

The time period measured between subsequent Hall sensor states is inversely proportional to the speed of the motor; therefore, a proportionality constant is needed. The PHASE_INC_CALC is a constant that is used to compute the phase increment from the average period.

EQUATION 2: PHASE INC CALC

$$PHASE_INC_CALC = \left(\frac{FCY}{Prescaler * PWM_Switching_Frequency} \right) \left(\frac{65536}{6} \right)$$

EQUATION 3: PHASE INCREMENT

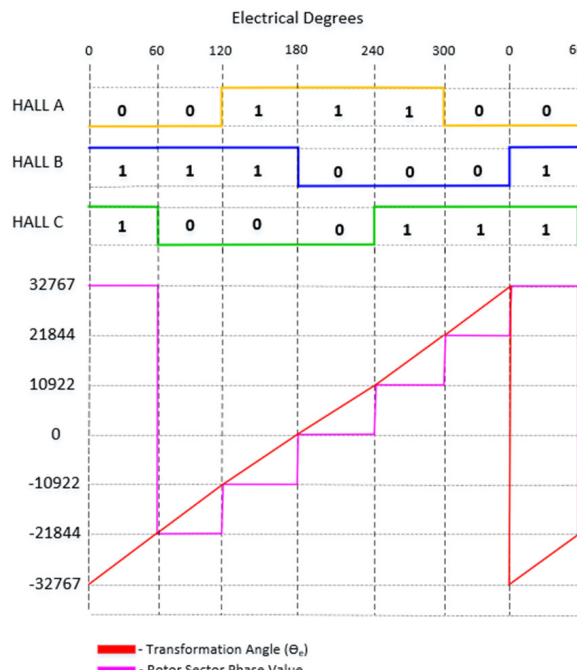
$$phaseInc = \left(\frac{PHASE_INC_CALC}{AveragePeriod} \right)$$

EQUATION 4: FINAL TRANSFORMATION ANGLE

$$\theta_{Electrical} = \theta_{Electrical} + phaseInc$$

From the equation above, the constant PHASE_INC_CALC is derived from dividing the SCCP Timer clock by the Timer Prescaler and PWM switching frequency and multiplying the quotient by the equivalent phase value of 60-electrical degrees. The *phaseInc* variable is computed from dividing the PHASE_INC_CALC by the average period. The *phaseInc* value is used to increment the transformation angle in every ADC_ISR() cycle. The computed transformation angle reflects the electrical angle at a distinct moment in time. The process continues until another change notification interrupt event is serviced, and a new reference value is obtained. For a more elaborate illustration on the relationship among the sector number, rotor sector phase value and transformation angle, see the diagram in the following figure.

FIGURE 14: ROTOR ANGULAR POSITION



7.2 Speed Measurement

Due to motor mechanical construction and that the Hall effect sensors might not be perfectly placed at 120 degrees from each other, the time between the change of the Hall states is slightly different. For this reason, a single period capture is not sufficient to accurately calculate the speed. To complete a single electrical rotation, it will take six change notification interrupts. The period measured from those succeeding interrupts are integrated and used to calculate the speed. The following equation is used for calculating the raw speed.

EQUATION 5: SPEED CALCULATION

$$\text{calculatedSpeed} = \left(\frac{\text{SPEED_MULTI}}{\text{Period_Summation}} \right)$$

$$\text{where: SPEED_MULTI} = \left(\frac{\text{FCY} * 60}{\text{Timer_Prescaler}} \right)$$

The *Period_Summation* is a moving average summation that ensures that the *calculatedSpeed* will always be computed after every six change notification interrupts. The *calculatedSpeed* is filtered using the moving average filter to ensure that the measured speed is smooth and has no random noises.

The final output of the position and speed block are the measured speed and electrical angle that are fed to the PI control blocks.

8.0 FAULT DETECTION AND PROTECTION

The application firmware is equipped with fault detection and protection against shoot-through, overcurrent, overtemperature and undervoltage. These unwanted events may damage the motor and motor drivers, thus it is recommended to prevent them.

8.1 Shoot-through

It is a failure event when two complementary switches in a voltage source inverter are turned on simultaneously, consequently short-circuiting the supply.

The PWM peripheral has the dead-time generator that is applied in both the rising and falling edges of the PWM signals to prevent shoot-through. The dead time lasts for 1 μ s, ensuring that discharge or turn-off delay time does not falsely switch ON the complementary switches simultaneously.

8.2 Overcurrent Protection

Overcurrent describes a sharp and fast rise in current over a short period of time. It can be caused by improper commutation, excessive load, line-to-ground or line-to-line faults. In this condition, the value of the current is far greater than the nominal line current and may result in the circuit overheating.

The current is monitored through the current-sensing circuits connected to the phase A of the motor. The resistor R_{SHUNT} is tapped at the low side of the inverter. The voltage across R_{SHUNT} reflects the current that flows through the inverter. The DSCs internal op amp is utilized for measuring and conditioning the voltage signal. The output of the internal op amp is fed to the non-inverting input of comparator with DAC. The DAC is connected to the inverting input of the Comparator and sets the reference value. The DAC has a 12-bit resolution that can provide 5% to 95% of AVDD. The measured voltage signal is continuously compared to the reference voltage set by the DAC. If the voltage signal goes higher than the voltage set by the DAC for 100 μ s, the PWM drivers are disabled and the motor is stopped.

8.3 Overtemperature Protection

The operating ambient temperature range of dsPIC33CK64MP105 is from -40 to +85°C. The overtemperature detection for the microcontroller is done through the Temperature Sensor tied to AN19 pin of dsPIC. The diode in the temperature sensor has a negative temperature coefficient. The ADC is used to monitor the die temperature through channel AN19. The temperature limit is set depending on the measured voltage at normal operation and adjusted on the ambient temperature range. At 25°C, the measured ADC value is 240. The formula for getting the ADC Value is expressed in the following equation.

EQUATION 6: EQUIVALENT DIGITAL VALUE OF SENSED TEMPERATURE

$$ADC\ Result = \left(\frac{V_{temp}}{V_{DD}} \right) (2^n - 1)$$

Rearranging the previous formula in the previous equation leads to the following equation.

EQUATION 7: VOLTAGE MEASURED AT ROOM TEMPERATURE

$$V_{temp} = \frac{ADC\ Result * V_{DD}}{2^n - 1}$$
$$V_{temp} = \frac{240 * 3.3}{2^{10} - 1} = 0.77419$$

This V_{temp} @ 25°C is used as the reference voltage in which the change in voltage across the diode with the temperature coefficient of -1.5 mV / °C will be added or deducted depending on the rise or fall of the temperature. The new V_{temp} is computed using the following equation.

EQUATION 8: VOLTAGE MEASURED AT ANY TEMPERATURE

$$V_{temp} = 0.77419 + (Temp_{new} - 25)(-1.5)$$

The fault protection is designed to shut down the system if the temperature rises to 57°C or equivalent to the ADC value of 225 because it is recommended that the battery of the electric scooter not operate in a temperature greater than 60°C or equivalent to the ADC value of 224.

8.4 Undervoltage Protection

Undervoltage is defined as a condition in which the voltage drops to less than 90% of the rated voltage for at least one minute.

The undervoltage in V_{BUS} is directly monitored by the controller using the $V_{BUS}/16$ signal, which has a direct connection to the dsPIC AN15 channel input. The routine used for monitoring the bus voltage is within the Interrupt Service Routine used for driving the motor. It is checked for every 20 μ s. To avoid false triggers for undervoltage, a counter is used for counting the elapsed time for the undervoltage. If the counter exceeds 1 minute, the undervoltage fault will be activated, which causes the system to be disabled.

It is recommended not to let the battery drop below 70%, so the controller undervoltage protection would be 0.7 V_{BAT} . Using the following equation, the voltage limit is computed.

EQUATION 9: VOLTAGE LIMIT

$$Voltage\ Limit = \frac{V_{BUS}(2^n - 1)}{16V_{DD}}$$

where: $V_{BUS} = 0.7V_{BAT}$

9.0 APPLICATION OF SENSORED FOC IN ELECTRIC SCOOTER

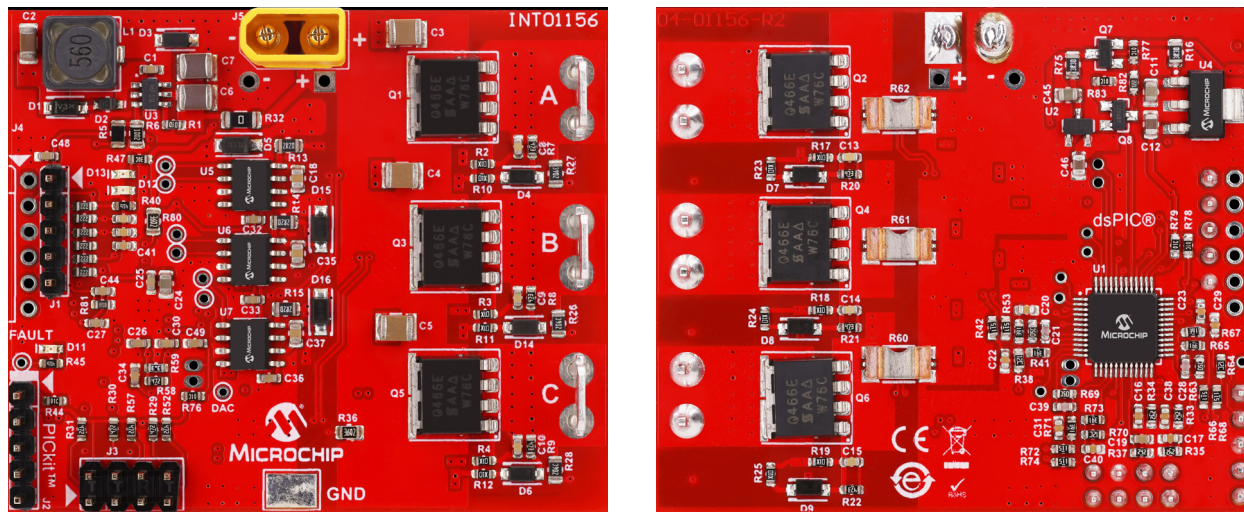
In recent years, the use of electric two-wheelers, such as the electric scooter, as a means of personal transportation became widespread. An electric scooter is composed of a battery, battery charger, motor, motor driver, DC-DC converter, intelligent controller and other accessories.

The motor is fixed in the hub of the wheel. The sensored BLDC motor has a very similar construction with a permanent magnet synchronous motor used as a hub motor. The reason for choosing BLDC is its compactness, low maintenance, and noiseless operation. The Hall effect sensors are already included in the construction of the motor. The hub motor typical voltage is 36V – 42V, with the speed ranging from 150 RPM to 650 RPM or 5 kph to 25 kph.

The sensored FOC technique is very suitable for driving the electric scooter because it provides an efficient way to control the BLDC motor in adjustable speed drive applications. The FOC technique improves the torque response and dynamic speed accuracy. The sensored nature of the solution makes it appropriate for the high precision drive of the electric scooter hub motor.

With an increasing demand for electric scooters, a board was developed to cater to the need for intelligent control of electric scooters. The electric scooter board was developed with a DC-DC converter, intelligent controller and motor driver with a fully protected power stage. The board only requires the throttle signal, battery and battery charger to completely control the electric scooter. The board was used in testing the solution discussed in this application note. The reference design of the board was released in a separate document. The figure below shows the front and back of the electric scooter board.

FIGURE 15: FRONT AND BACK BOARD PICTURES



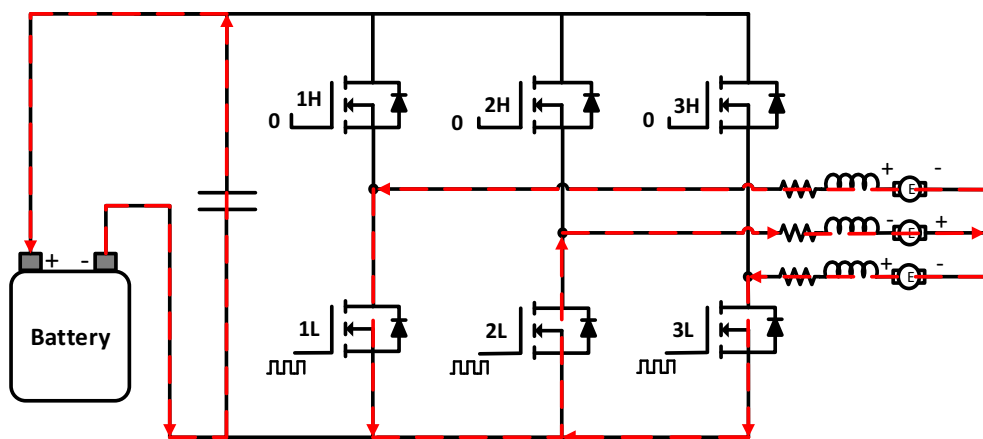
The stopping of the motor is an important consideration in controlling the electric scooter. Regenerative braking is an additional feature used for speeding up the deceleration and extending the battery life.

9.1 Regenerative Braking

Regenerative braking is the process of using a motor in motion as a generator, consequently, making the motor slow down. The energy recovered in the process is stored back to the battery. The energy can only be stored when the Back EMF generated by the BLDC motor is greater than the battery voltage. For practical application, regenerative braking is preferred at high-speed motor operation.

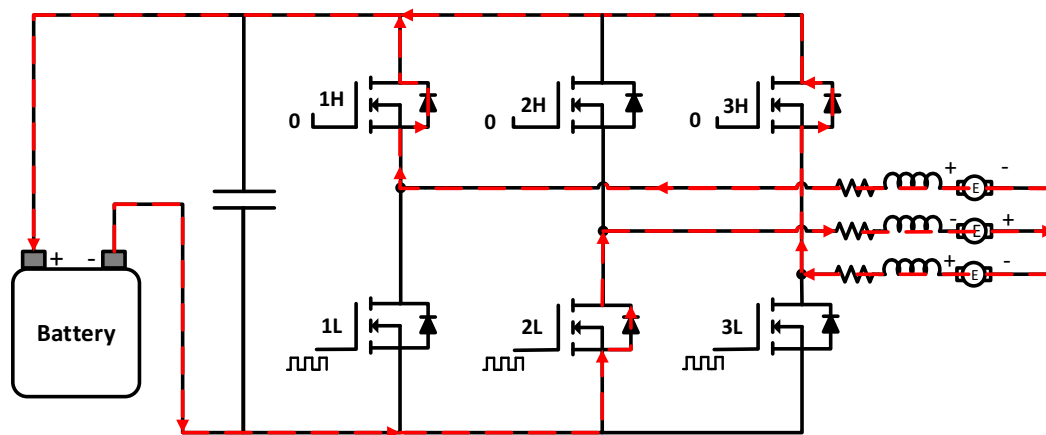
The three-switch regenerative braking method is used in this application. An additional pin is used as an input for processing the signal coming from the brake lever. The braking routine is included in the interrupt service routine used for driving the motor. When a brake signal is sensed, the PWM signal is applied to the low side switches of the inverter while the high side switches are turned off, as shown in the following figure.

FIGURE 16: LOW SIDE SWITCHES ARE MODULATED



This switch configuration allows the converted electrical energy from the rotating motor to be boosted to a higher voltage than the DC bus voltage. The second step in the process is turning off the low side switches, letting the current flow back to the source through the MOSFET body diode, as shown in the following figure. The boosted voltage is, then, stored back to the battery.

FIGURE 17: LOW SIDE SWITCHES ARE OFF



10.0 TESTING ON THE ELECTRIC SCOOTER BOARD

This section presents the results of testing the sensored FOC drive in an electric scooter at no load condition. This illustrates the rotor angular position, the SVM line-to-ground voltages and the SVM line-to-line voltages. The diagrams and graphs are captured using X2CScope, a virtual oscilloscope tool that allows run-time debugging and data visualization.

FIGURE 18: ROTOR ANGULAR POSITION AND SECTOR PHASE VALUE

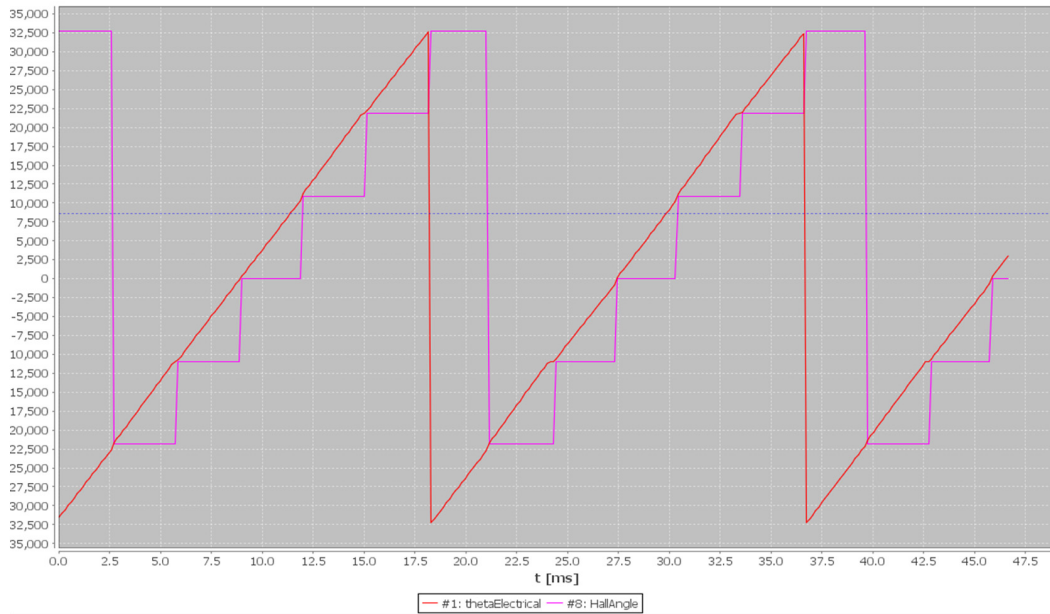


FIGURE 19: SVM LINE-TO-GROUND VOLTAGES

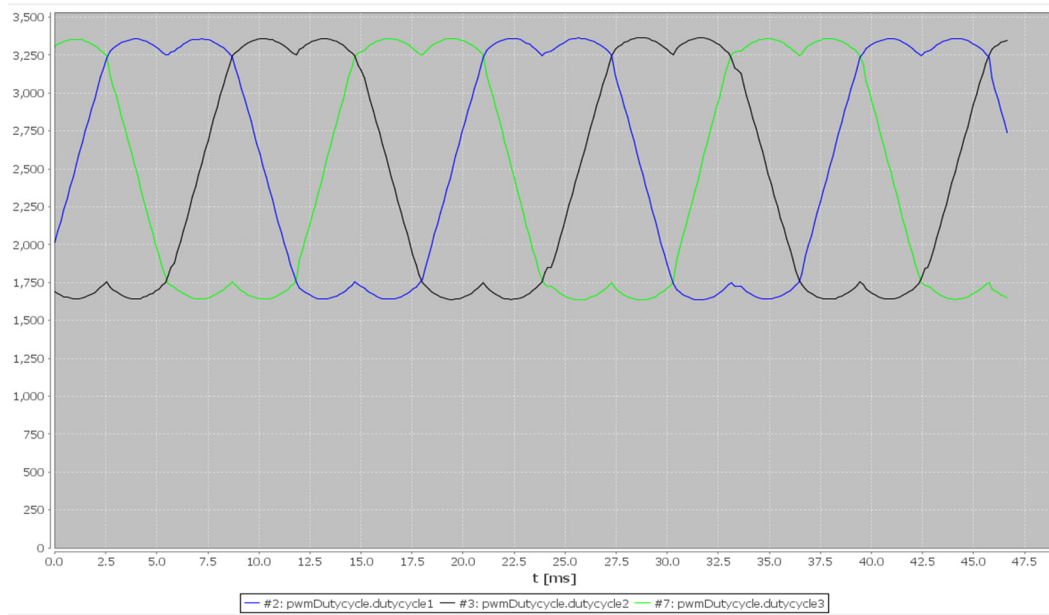
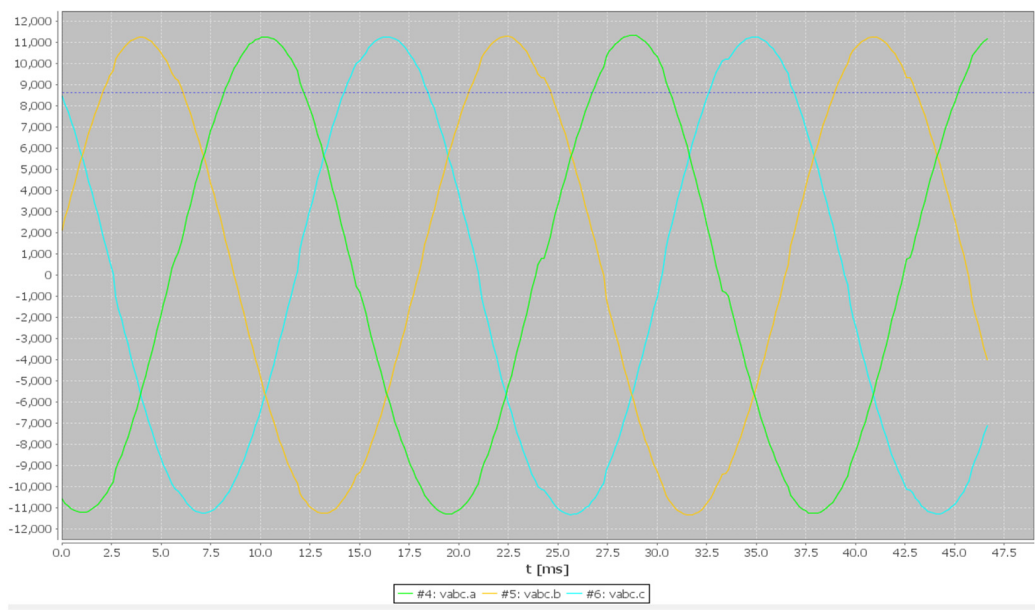


FIGURE 20: SVM LINE-TO-LINE VOLTAGES

11.0 CONCLUSION

The sensored FOC based on Hall effect sensor achieved the high-precision speed and position control of the 3-Phase BLDC motor through developing a high-resolution algorithm out of Hall effect sensor states. The 16-bit Microchip dsPIC33CK DSC efficiently used its DSP for executing the FOC algorithm and its on-chip peripherals for a cost-effective solution. The solution presented in this application note effectively drives the 3-Phase BLDC hub motor of the electric scooter. Fault protection was added to the system to ensure that unwanted events that can cause system failure can be readily detected and stop the system's operation.

APPENDIX A: SOURCE CODE LISTING

The latest software version can be downloaded from the Microchip website (www.microchip.com). The user will find the source code appended to the electronic version of this application note.

APPENDIX B: REVISION HISTORY

Revision	Date	Section	Description
A	07/2021	Document	Initial release

Note the following details of the code protection feature on Microchip devices:

- Microchip products meet the specifications contained in their particular Microchip Data Sheet.
- Microchip believes that its family of products is secure when used in the intended manner and under normal conditions.
- There are dishonest and possibly illegal methods being used in attempts to breach the code protection features of the Microchip devices. We believe that these methods require using the Microchip products in a manner outside the operating specifications contained in Microchip's Data Sheets. Attempts to breach these code protection features, most likely, cannot be accomplished without violating Microchip's intellectual property rights.
- Microchip is willing to work with any customer who is concerned about the integrity of its code.
- Neither Microchip nor any other semiconductor manufacturer can guarantee the security of its code. Code protection does not mean that we are guaranteeing the product is "unbreakable." Code protection is constantly evolving. We at Microchip are committed to continuously improving the code protection features of our products. Attempts to break Microchip's code protection feature may be a violation of the Digital Millennium Copyright Act. If such acts allow unauthorized access to your software or other copyrighted work, you may have a right to sue for relief under that Act.

Information contained in this publication is provided for the sole purpose of designing with and using Microchip products. Information regarding device applications and the like is provided only for your convenience and may be superseded by updates. It is your responsibility to ensure that your application meets with your specifications.

THIS INFORMATION IS PROVIDED BY MICROCHIP "AS IS". MICROCHIP MAKES NO REPRESENTATIONS OR WARRANTIES OF ANY KIND WHETHER EXPRESS OR IMPLIED, WRITTEN OR ORAL, STATUTORY OR OTHERWISE, RELATED TO THE INFORMATION INCLUDING BUT NOT LIMITED TO ANY IMPLIED WARRANTIES OF NON-INFRINGEMENT, MERCHANTABILITY, AND FITNESS FOR A PARTICULAR PURPOSE OR WARRANTIES RELATED TO ITS CONDITION, QUALITY, OR PERFORMANCE.

IN NO EVENT WILL MICROCHIP BE LIABLE FOR ANY INDIRECT, SPECIAL, PUNITIVE, INCIDENTAL OR CONSEQUENTIAL LOSS, DAMAGE, COST OR EXPENSE OF ANY KIND WHATSOEVER RELATED TO THE INFORMATION OR ITS USE, HOWEVER CAUSED, EVEN IF MICROCHIP HAS BEEN ADVISED OF THE POSSIBILITY OR THE DAMAGES ARE FORESEEABLE. TO THE FULLEST EXTENT ALLOWED BY LAW, MICROCHIP'S TOTAL LIABILITY ON ALL CLAIMS IN ANY WAY RELATED TO THE INFORMATION OR ITS USE WILL NOT EXCEED THE AMOUNT OF FEES, IF ANY, THAT YOU HAVE PAID DIRECTLY TO MICROCHIP FOR THE INFORMATION. Use of Microchip devices in life support and/or safety applications is entirely at the buyer's risk, and the buyer agrees to defend, indemnify and hold harmless Microchip from any and all damages, claims, suits, or expenses resulting from such use. No licenses are conveyed, implicitly or otherwise, under any Microchip intellectual property rights unless otherwise stated.

Trademarks

The Microchip name and logo, the Microchip logo, Adaptec, AnyRate, AVR, AVR logo, AVR Freaks, BesTime, BitCloud, chipKIT, chipKIT logo, CryptoMemory, CryptoRF, dsPIC, FlashFlex, flexPWR, HELDO, IGLOO, JukeBlox, KeeLoq, Kleer, LANCheck, LinkMD, maXStylus, maXTouch, MediaLB, megaAVR, Microsemi, Microsemi logo, MOST, MOST logo, MPLAB, OptoLyzer, PackeTime, PIC, picoPower, PICSTART, PIC32 logo, PolarFire, Prochip Designer, QTouch, SAM-BA, SenGenuity, SpyNIC, SST, SST Logo, SuperFlash, Symmetricom, SyncServer, Tachyon, TimeSource, tinyAVR, UNI/O, Vectron, and XMEGA are registered trademarks of Microchip Technology Incorporated in the U.S.A. and other countries.

AgileSwitch, APT, ClockWorks, The Embedded Control Solutions Company, EtherSynch, FlashTec, Hyper Speed Control, HyperLight Load, IntelliMOS, Libero, motorBench, mTouch, Powermite 3, Precision Edge, ProASIC, ProASIC Plus, ProASIC Plus logo, Quiet-Wire, SmartFusion, SyncWorld, Temux, TimeCesium, TimeHub, TimePictra, TimeProvider, WinPath, and ZL are registered trademarks of Microchip Technology Incorporated in the U.S.A.

Adjacent Key Suppression, AKS, Analog-for-the-Digital Age, Any Capacitor, AnyIn, AnyOut, Augmented Switching, BlueSky, BodyCom, CodeGuard, CryptoAuthentication, CryptoAutomotive, CryptoCompanion, CryptoController, dsPICDEM, dsPICDEM.net, Dynamic Average Matching, DAM, ECAN, Espresso T1S, EtherGREEN, IdealBridge, In-Circuit Serial Programming, ICSP, INICnet, Intelligent Paralleling, Inter-Chip Connectivity, JitterBlocker, maxCrypto, maxView, memBrain, Mindi, MiWi, MPASM, MPF, MPLAB Certified logo, MPLIB, MPLINK, MultiTRAK, NetDetach, Omniscient Code Generation, PICDEM, PICDEM.net, PICkit, PICtail, PowerSmart, PureSilicon, QMatrix, REAL ICE, Ripple Blocker, RTAX, RTG4, SAM-ICE, Serial Quad I/O, simpleMAP, SimpliPHY, SmartBuffer, SMART-I.S., storClad, SQL, SuperSwitcher, SuperSwitcher II, Switchtec, SynchroPHY, Total Endurance, TSHARC, USBCheck, VariSense, VectorBlox, VeriPHY, ViewSpan, WiperLock, XpressConnect, and ZENA are trademarks of Microchip Technology Incorporated in the U.S.A. and other countries.

SQTP is a service mark of Microchip Technology Incorporated in the U.S.A.

The Adaptec logo, Frequency on Demand, Silicon Storage Technology, and Symmcom are registered trademarks of Microchip Technology Inc. in other countries.

GestIC is a registered trademark of Microchip Technology Germany II GmbH & Co. KG, a subsidiary of Microchip Technology Inc., in other countries.

All other trademarks mentioned herein are property of their respective companies.

© 2021, Microchip Technology Incorporated, All Rights Reserved.

ISBN: 978-1-5224-8391-5

For information regarding Microchip's Quality Management Systems, please visit www.microchip.com/quality.



MICROCHIP

Worldwide Sales and Service

AMERICAS

Corporate Office
2355 West Chandler Blvd.
Chandler, AZ 85224-6199
Tel: 480-792-7200
Fax: 480-792-7277
Technical Support:
<http://www.microchip.com/support>
Web Address:
www.microchip.com

Atlanta

Duluth, GA
Tel: 678-957-9614
Fax: 678-957-1455

Austin, TX

Tel: 512-257-3370

Boston

Westborough, MA
Tel: 774-760-0087
Fax: 774-760-0088

Chicago

Itasca, IL
Tel: 630-285-0071
Fax: 630-285-0075

Dallas

Addison, TX
Tel: 972-818-7423
Fax: 972-818-2924

Detroit

Novi, MI
Tel: 248-848-4000

Houston, TX

Tel: 281-894-5983

Indianapolis

Noblesville, IN
Tel: 317-773-8323
Fax: 317-773-5453
Tel: 317-536-2380

Los Angeles

Mission Viejo, CA
Tel: 949-462-9523
Fax: 949-462-9608
Tel: 951-273-7800

Raleigh, NC

Tel: 919-844-7510

New York, NY

Tel: 631-435-6000

San Jose, CA

Tel: 408-735-9110
Tel: 408-436-4270

Canada - Toronto

Tel: 905-695-1980
Fax: 905-695-2078

ASIA/PACIFIC

Australia - Sydney
Tel: 61-2-9868-6733
China - Beijing
Tel: 86-10-8569-7000
China - Chengdu
Tel: 86-28-8665-5511
China - Chongqing
Tel: 86-23-8980-9588
China - Dongguan
Tel: 86-769-8702-9880
China - Guangzhou
Tel: 86-20-8755-8029
China - Hangzhou
Tel: 86-571-8792-8115
China - Hong Kong SAR
Tel: 852-2943-5100
China - Nanjing
Tel: 86-25-8473-2460
China - Qingdao
Tel: 86-532-8502-7355
China - Shanghai
Tel: 86-21-3326-8000
China - Shenyang
Tel: 86-24-2334-2829
China - Shenzhen
Tel: 86-755-8864-2200
China - Suzhou
Tel: 86-186-6233-1526
China - Wuhan
Tel: 86-27-5980-5300
China - Xian
Tel: 86-29-8833-7252
China - Xiamen
Tel: 86-592-2388138
China - Zhuhai
Tel: 86-756-3210040

ASIA/PACIFIC

India - Bangalore
Tel: 91-80-3090-4444
India - New Delhi
Tel: 91-11-4160-8631
India - Pune
Tel: 91-20-4121-0141
Japan - Osaka
Tel: 81-6-6152-7160
Japan - Tokyo
Tel: 81-3-6880- 3770
Korea - Daegu
Tel: 82-53-744-4301
Korea - Seoul
Tel: 82-2-554-7200
Malaysia - Kuala Lumpur
Tel: 60-3-7651-7906
Malaysia - Penang
Tel: 60-4-227-8870
Philippines - Manila
Tel: 63-2-634-9065
Singapore
Tel: 65-6334-8870
Taiwan - Hsin Chu
Tel: 886-3-577-8366
Taiwan - Kaohsiung
Tel: 886-7-213-7830
Taiwan - Taipei
Tel: 886-2-2508-8600
Thailand - Bangkok
Tel: 66-2-694-1351
Vietnam - Ho Chi Minh
Tel: 84-28-5448-2100

EUROPE

Austria - Wels
Tel: 43-7242-2244-39
Fax: 43-7242-2244-393
Denmark - Copenhagen
Tel: 45-4485-5910
Fax: 45-4485-2829
Finland - Espoo
Tel: 358-9-4520-820
France - Paris
Tel: 33-1-69-53-63-20
Fax: 33-1-69-30-90-79
Germany - Garching
Tel: 49-8931-9700
Germany - Haan
Tel: 49-2129-3766400
Germany - Heilbronn
Tel: 49-7131-72400
Germany - Karlsruhe
Tel: 49-721-625370
Germany - Munich
Tel: 49-89-627-144-0
Fax: 49-89-627-144-44
Germany - Rosenheim
Tel: 49-8031-354-560
Israel - Ra'anana
Tel: 972-9-744-7705
Italy - Milan
Tel: 39-0331-742611
Fax: 39-0331-466781
Italy - Padova
Tel: 39-049-7625286
Netherlands - Drunen
Tel: 31-416-690399
Fax: 31-416-690340
Norway - Trondheim
Tel: 47-7288-4388
Poland - Warsaw
Tel: 48-22-3325737
Romania - Bucharest
Tel: 40-21-407-87-50
Spain - Madrid
Tel: 34-91-708-08-90
Fax: 34-91-708-08-91
Sweden - Gothenberg
Tel: 46-31-704-60-40
Sweden - Stockholm
Tel: 46-8-5090-4654
UK - Wokingham
Tel: 44-118-921-5800
Fax: 44-118-921-5820